

## Original Article

# A novel approach for the annulus needle puncture model of intervertebral disc degeneration in rabbits

Tao Lei<sup>1</sup>, Yuan Zhang<sup>1</sup>, Qiang Zhou<sup>1</sup>, Xiaoji Luo<sup>1</sup>, Ke Tang<sup>1</sup>, Rongsheng Chen<sup>2</sup>, Chang Yu<sup>1</sup>, Zhengxue Quan<sup>1</sup>

Departments of <sup>1</sup>Orthopedic Surgery, <sup>2</sup>Radiology, The First Affiliated Hospital of Chongqing Medical University, Chongqing 400016, China

Received September 22, 2016; Accepted February 9, 2017; Epub March 15, 2017; Published March 30, 2017

**Abstract:** Objective: To create the rabbit animal model of intervertebral disc (IVD) degeneration by the annulus needle puncture technique through a novel transabdominal approach. Methods: Thirteen New Zealand White rabbits underwent annular puncture at the L3/4, L4/5, and L5/6 discs through a transabdominal approach. For a longitudinal study to assess changes in disc height over time, serial X-rays, T2-weighted magnetic resonance imaging (MRI) (T2WI), and T2 mapping MRI were performed pre-operation and at 2, 4, and 6 weeks after puncture. Three rabbits were randomly selected for histological evaluation at 4 weeks post-operation. In addition, the remaining rabbits underwent a second surgery at 6 weeks after puncture. Results: All rabbits underwent the initial and second surgeries successfully without nerve-related complications. The operations had no significant effects on the rabbit body weight, and partial mild intra-abdominal adhesions were found in only 1 rabbit. The punctured discs were confirmed to be those of interest post-surgery and displayed progressive degeneration in disc height index (%), T2WI, and T2 relaxation time over time. At 4 weeks after puncture, a histological analysis revealed notochordal cell loss from the nucleus pulposus, fibrocartilage filling the nucleus pulposus space, and annulus fibrosus disorganization. Conclusion: The annular needle puncture model established through a transabdominal approach, which demonstrates better visualization, exact identification, consistent degeneration degrees and minimal complications, is radiologically and histologically consistent with human IVD degeneration. T2 mapping MRI can quantitatively discriminate between grades of mild degeneration.

**Keywords:** Animal model, intervertebral disc degeneration, annular puncture, transabdominal approach, T2 mapping

## Introduction

Back pain is a common clinical problem that is highly prevalent in adults and has a major socioeconomic impact [1]. Intervertebral disc (IVD) degeneration is a major contributor to low back pain [2]. Current treatment options include both conservative and surgical measures. Unfortunately, conservative treatments are often unsuccessful in alleviating patient symptoms and preventing symptom recurrence, whereas surgical methods are highly invasive, costly, and associated with significant complications (e.g., nonunion, infections, implant breakage [3], and adjacent segment disease [4]). Excitingly, recent advances in molecular biology may enable the development of biological treatment strategies to repair or regenerate degenerated IVDs biologically. Such strategies

are currently being investigated as potential and promising treatment methods [5].

Animal models are essential for the transition from scientific concepts to clinical applications. In addition, the safety and effectiveness of experimental paradigms need to be validated using appropriate animal models. Recently, multiple approaches to create animal models of IVD degeneration have been reported [6]. Common approaches to model development have been either to study animal models in which disc degeneration occurs naturally (e.g., the sand rat [7]) or to cause a more rapid form of disc degeneration via an artificial intervention (e.g., by applying mechanical loads to discs using an external compression device [8, 9] or applying biochemicals [10, 11]). The above methods are sophisticated, costly and may require

## A novel method for establishing the degenerative IVD model



**Figure 1.** Selected instruments, including two blade holders and an 18-gauge lumbar puncture needle with an artificial sheath trimmed to a depth of 5 mm.

special equipment and materials. In addition, it is possible to introduce confounding factors, which cause difficulties in analyzing the results. The annulus needle puncture model via a retroperitoneal approach provides relatively slow, reproducible, and progressive disc degeneration [12] and is widely used. However, this approach has many complications (e.g., deep incision, worse visualization, bilateral hind leg paralysis, nerve root injury, and incorrect identification of IVDs of interest) [13, 14].

We have been working to develop an easier method for establishing the annulus needle puncture model of IVD degeneration with fewer side effects. In this present study, we provide a transabdominal approach for establishing this model with magnetic resonance imaging (MRI), X-ray and histological validation.

### Materials and methods

#### *Animal preparation*

With approval (Grant No. 2016-60) from the Committee on the Ethics of the First Affiliated Hospital of Chongqing Medical University, thirteen New Zealand White Rabbits, weighing approximately 2.0 to 2.5 kg, correlating to an age of approximately 3 months, were purchased and housed in the Animal Center of Chongqing Medical University. Preoperative lateral radiography and MRI of the lumbar spine were performed to serve as a baseline for future comparisons, determine the spinal anatomy for appropriate IVD level selection, and monitor disc degeneration progression. The rabbits

were allowed to acclimatize for five days after the first X-ray and MRI. No food was given the day before the procedure, and the rabbits were administered prophylactic antibiotics intramuscularly (benzylpenicillin sodium, 200,000 IU/kg, North China Pharmaceutical Co., Ltd., China) half an hour before surgery. Immediately afterward, each rabbit was anesthetized with an intravenous injection of phenobarbital sodium salt (30 mg/kg, Merck, Shanghai, China). If necessary, additional

anesthetic was administered during surgery. The ventral side was then shaved from approximately the lowest rib to the iliac crest level. The rabbit was then placed in the operating suite in the supine position. The skin was prepared for aseptic surgery via a triple rinse with povidone iodine solution. The animal was then draped to isolate the prepared area.

#### *Required instruments*

The following instruments were required: a no. 15 scalpel and two blade holders; an 18-gauge lumbar puncture needle with an artificial sheath trimmed to a depth of 5 mm; forceps; hemostats; scissors; and sterile gauze (**Figure 1**).

#### *Exposure and localization of the IVDs of interest*

A 10-cm ventral median skin incision was made between the subcostal and iliac crest level (**Figure 2A**). The abdominal wall was then incised layer by layer for entry into the peritoneal cavity. Care was taken to avoid injuring the abdominal organs, particularly the intestines, which were subsequently pulled to the right gently. The posterior peritoneum was exposed (**Figure 2B**) and then incised between the left ureter and abdominal aorta. In our experience, the left renal vein crossed the L3 vertebral body; therefore, we could use palpation to find the L3/4 IVD, which is the first disc below the left renal vein, and it could be atraumatically exposed by bluntly manipulating the prevertebral muscles with the blade holder. The L4/5, L5/6 and L6/7 discs were exposed in the same

## A novel method for establishing the degenerative IVD model

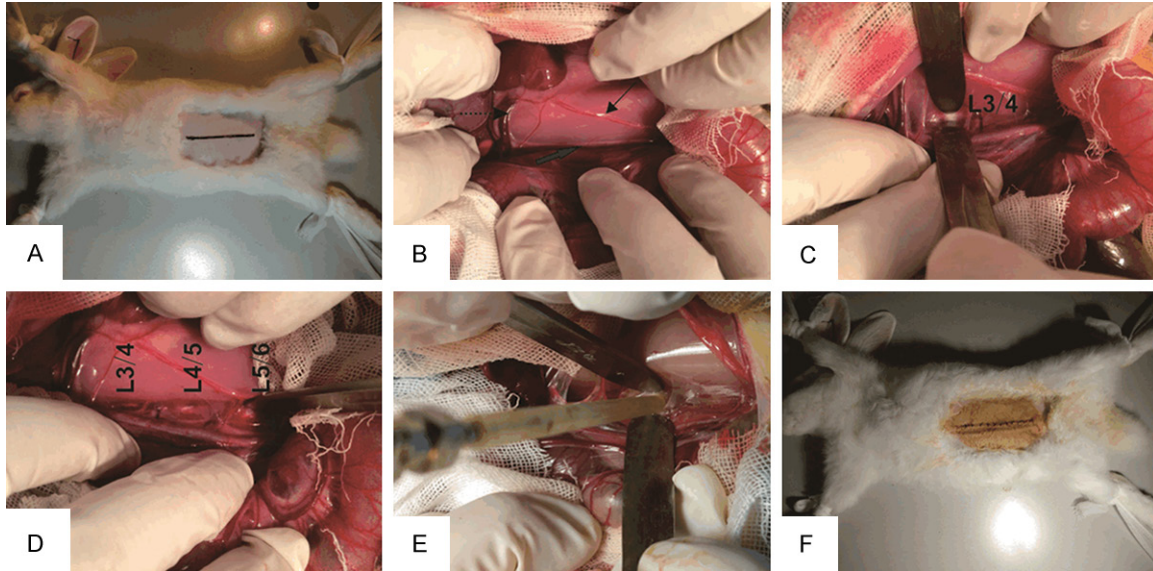


**Figure 2.** Establishment of the annulus needle puncture model of lumbar IVD degeneration via the transabdominal approach. The shaved region and skin incision (solid line) (A). Exposure of the posterior peritoneum, the left renal vein (dashed arrow), the left ureter (solid arrow) and the abdominal aorta (thick arrow) (B). Exposure of the L3/4, L4/5, L5/6 IVDs (C, D). Induction of IVD degeneration by inserting the needle vertically (E). Closure of the abdominal cavity (F).

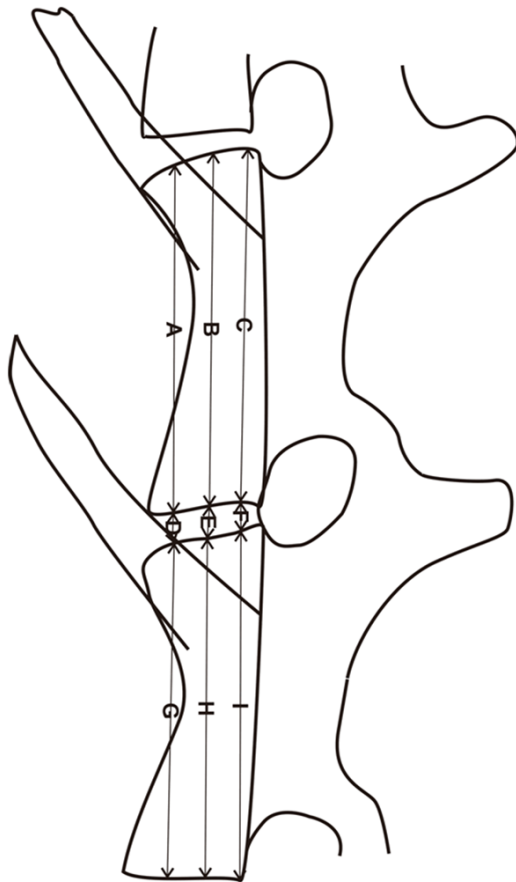


**Figure 3.** A schematic representation of how the DHIs were measured.

way and were validated by X-ray and MRI (**Figure 2C, 2D**).

### *Induction of IVD degeneration*

Once the IVDs of interest were identified and exposed, the needle was inserted vertically at the center of the annulus fibrosus (AF) anterior aspect into the nucleus pulposus (NP) and held for 5 seconds [12] (**Figure 2E**). The depth of the needle puncture was controlled to be exactly 5 mm by a hand-made sheath (**Figure 1**). A small amount of NP tissue automatically flowed out when the needle was withdrawn, and the puncture procedure was then repeated at the two other IVDs.

### *Closure and recovery*

It was not necessary to close the posterior peritoneum. The intestines were replaced into the abdominal cavity after the operative region was determined to exhibit no bleeding. The layers of the abdominal wall were then closed in an interrupted fashion with 4-0 non-absorbable braided sutures (**Figure 2F**). The rabbits were allowed cage activity ad libitum, and the diet, incision, and posterior limb activity were carefully observed after the operation. Additionally, prophylactic antibiotics (benzylpenicillin sodium, 200,000 IU/kg) were administered for 72 hours postoperatively.

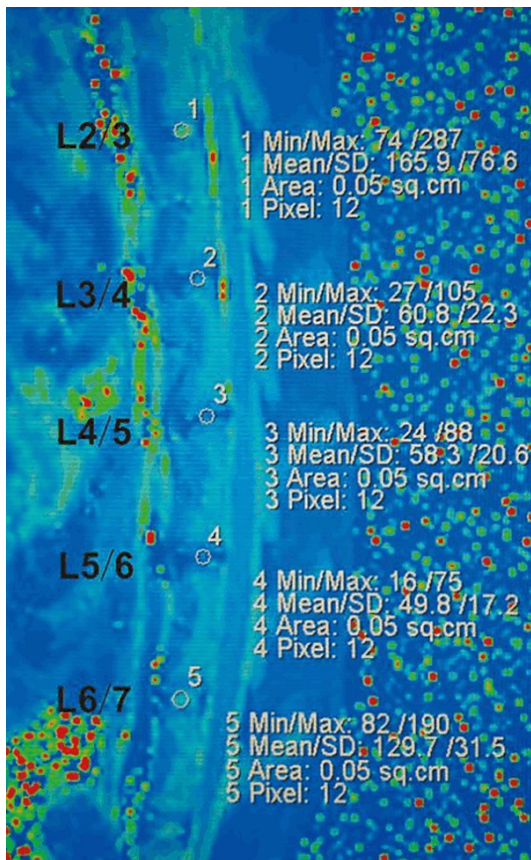


**Figure 4.** A representative color map produced by T2 mapping MRI. T2 relaxation times can be obtained by using syngo fastView software.

#### Radiological evaluation

Subsequently, the rabbits were anesthetized by an intravenous injection of phenobarbital sodium salt (30 mg/kg). Lateral plane radiographs obtained pre-operation and at each time point (2, 4, and 6 weeks post-operation) were digitalized. IVD heights were measured and expressed as the disc height index (DHI) using the method reported by Masuda et al. [12]. The average DHI was calculated by averaging the measurements obtained from the anterior, middle, and posterior portions of each IVD and dividing that by the average of adjacent vertebral body heights (**Figure 3**). Changes in the DHI were expressed as % DHI and normalized to the measured preoperative IVD height (% DHI=post-operation DHI/pre-operation DHI × 100).

Immediately after the radiography, MRI was performed on all rabbits using a 1.5-T imager with a quadrature extremity coil receiver (MAGETOM ESSENZA 1.5T, SIEMENS, Germany).

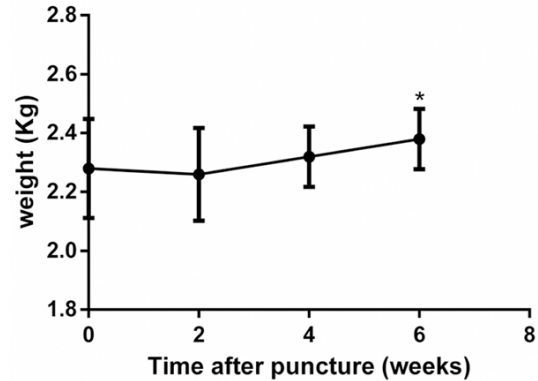


**Figure 5.** Change in weight over time after needle puncture. The average body weight at 6 weeks, but not 2 weeks or 4 weeks, after puncture was significantly greater than that before the operation (\* $P=0.042$ ).

T2-weighted sections of the median sagittal plane were obtained using the following settings: a fast spin echo (SE) sequence with a TR (time to repetition) of 3,220 ms and a TE (time to echo) of 124 ms; a 256 (h) × 166 (v) matrix; a field of view of 170 mm; and 1 average. The section thickness was 2 mm with a 0.5-mm gap. T2 relaxation time measurements were prepared by a multi-echo SE sequence [15]. MRI T2 mapping utilizes the T2 relaxation time for quantifying the moisture content and collagen breakdown [16] and was performed using the following settings: a TR of 1300 ms; a TE of 11.9, 23.8, 35.7, 47.6, 59.5, 71.4, 83.3, 95.2, 107.1, and 119.0 ms; a 256 (h) × 256 (v) matrix; a field of view of 170 mm; and 2 averages. The section thickness was 2 mm with a 0.5-mm gap; the total scan time 8 min and 11 s.

The T2-weighted MRI scans were evaluated according to the modified Thompson classification based on changes in the degree and area of signal intensity from grades 1 to 4 (1, normal; 2, minimal decrease in signal intensity but obvious narrowing of high-signal area; 3, moderate decrease in signal intensity; and 4, severe decrease in signal intensity).

The T2 mapping MRI scans were processed using an image processing and analysis system, and the exact T2 relaxation time was obtained using syngo fastView software (**Figure 4**).

All images were independently interpreted by two orthopedic researchers who were blinded,

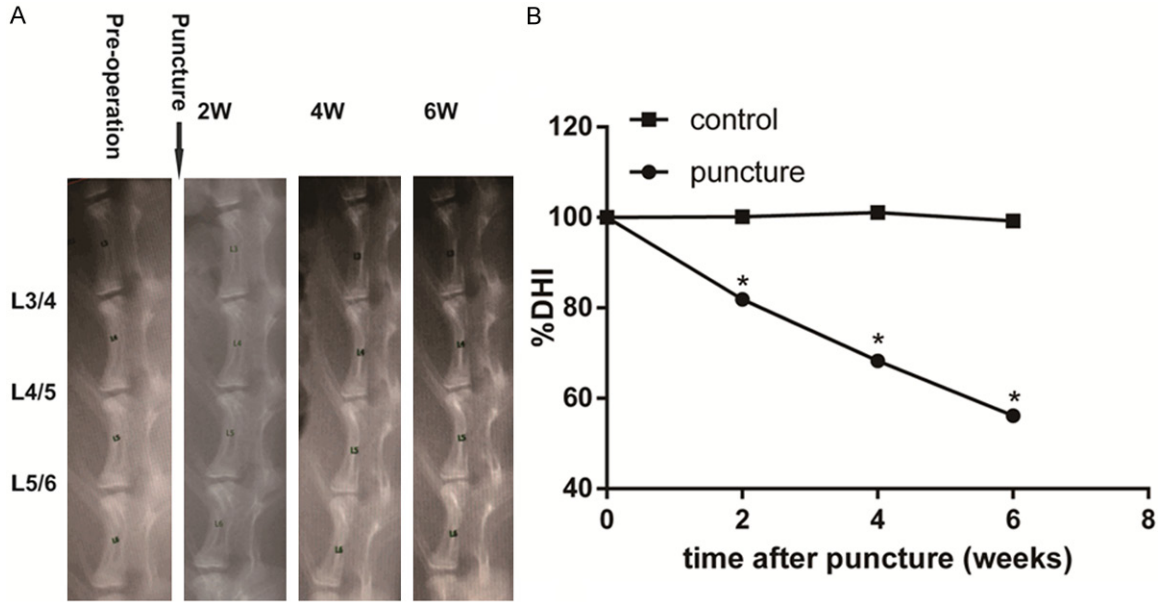


**Figure 6.** A. Representative X-rays of the lumbar region over time. B. Change in the DHI after needle puncture over time. A significant decrease was observed in the % DHI ( $P<0.01$ ) compared with that before the operation. There were no significant differences in % DHI at any time point in the control discs.

except for the initial validation study, to the following: study purpose, surgical procedure, and whether the films were pre- or post-surgery.

#### Histological evaluation

Three rabbits were euthanized at 4 weeks post-operation. After they were sacrificed, the IVD specimens were harvested for histological analysis. The tissues were fixed in 10% neutral-buffered formalin, decalcified in a 10% standard EDTA decalcifying solution (Boster Biological Technology Co., Ltd., Wuhan, China) for 3 or 4 weeks, paraffin-embedded, and sectioned to a thickness of 6  $\mu\text{m}$ . In addition, the sections were stained with hematoxylin and eosin (H&E) and qualitatively analyzed by light microscopy (Olympus BX51, Olympus, Japan) at magnifications ranging from 40-200X for evidence of changes in the NP and AF.

#### Statistical analysis

Statistical analysis was performed using IBM SPSS 22.0 software. The significance of differences among the weight (kg) and % DHI means at any time point was analyzed by repeated-measures analysis of variance (ANOVA) and Fisher's protected least significant difference (PLSD) post hoc test. The T2 relaxation times

(ms) with different degenerative grades were analyzed by one-way ANOVA and Fisher's PLSD post hoc test. All data are expressed as the mean  $\pm$  standard error. In addition, a Spearman rank correlation was performed to assess the correlation of the T2 values with the modified Thompson grades.  $P<0.05$  was defined as significant for all tests.

#### Results

Of the thirteen rabbits, no rabbits died during the operation, and the incisions healed well without becoming infected. All rabbits were observed to have a good diet and normal activity after the operation. Three rabbits were sacrificed for histological evaluations at 4 weeks after puncture. The weight of all rabbits was recorded over time to evaluate the effect of the operation on weight. The rabbit weight at 6 weeks, but not 2 or 4 weeks, after puncture was significantly greater than that before the operation ( $*P=0.042$ ) (Figure 5). Additionally, the second surgery (the injection of therapeutic factors) was successfully performed in the remaining 10 rabbits at 6 weeks after puncture. Mild partial intra-abdominal adhesions were observed in one rabbit during the injection surgery; thus, care should be taken to avoid injuring the intestines.

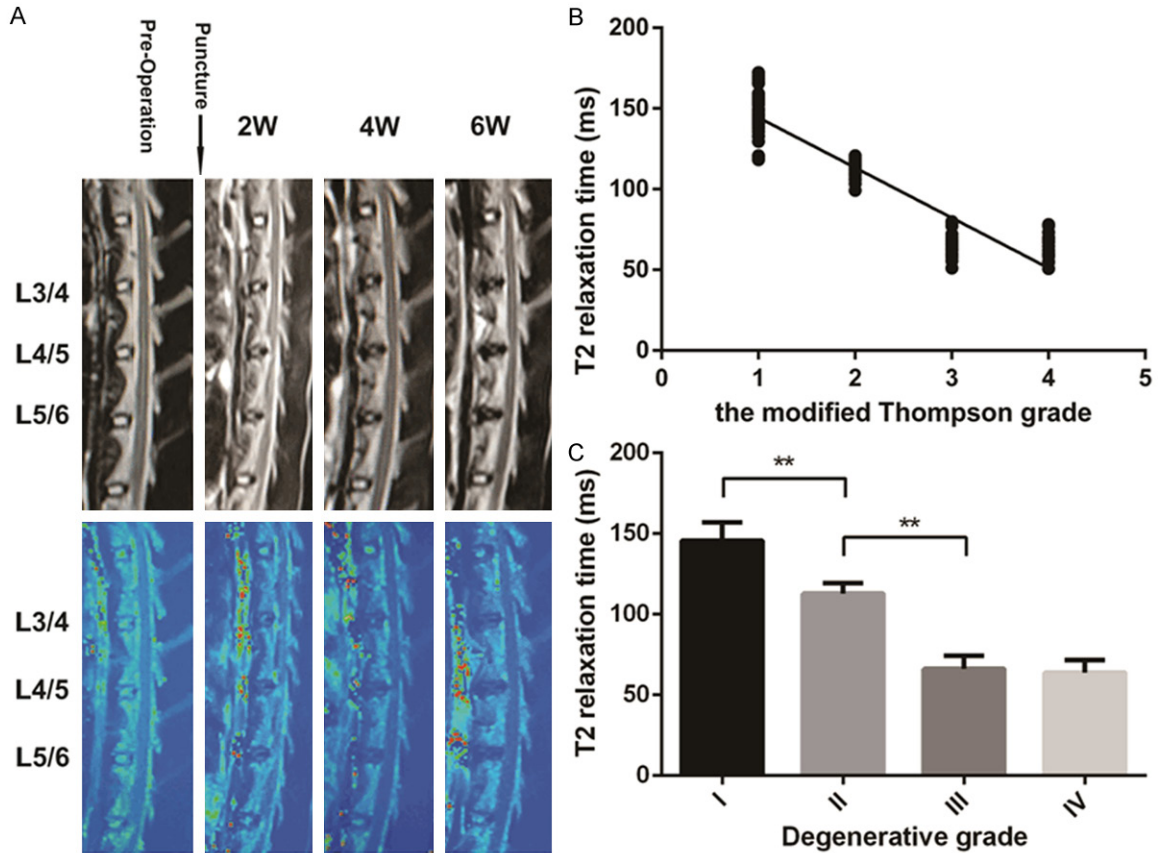


**Figure 7.** A. Representative T2WI and T2 mapping MRI scans of the lumbar region with different grades of degeneration over time. B. The correlation between T2 relaxation times (ms) and the modified Thompson grades ( $\rho=-0.916$ ,  $P<0.01$ ). C. T2 relaxation time (ms) in the NP per degenerative grade, as assessed using the modified Thompson classification system (\*\* $P<0.01$ ).

#### Imaging assessment

Generally, puncture with the 18-gauge needle resulted in a slow and progressive decrease in the % DHI. To assess disc height change over time, % DHI was calculated after 2, 4, and 6 weeks using the Picture Archiving and Communication Systems. In the control discs, there were no significant differences in % DHI at any time point. In contrast, the punctured discs showed significant narrowing of the disc space at 2 weeks (81.91%), 4 weeks (68.29%) and 6 weeks (56.17%) (all  $P<0.01$ ) (Figure 6B). Representative T2WI and T2 mapping MRI scans of the lumbar region with different degeneration grades over time are shown in Figure 7A. T2 values were obtained using image processing software (*syngo fastView*, SIEMENS) (Figure 4). The correlation between the T2 relaxation times in the NP and the modified Thompson grades was highly significant ( $\rho=-0.916$ ,  $P<0.01$ ) (Figure 7B). To examine whether T2 map-

ping could to discriminate among different grades of degeneration, mean T2 relaxation times in the NP were calculated per degenerative grade as assessed using the modified Thompson classification system. Figure 7C shows a downward trend of T2 values in the NP with increasing grade. The differences were significant between grades I and II ( $P<0.01$ ) and between grades II and III ( $P<0.01$ ). However, the differences between grades III and IV were not significant ( $P=0.368$ ). Apparently, T2 mapping could discriminate between grades of mild degeneration.

#### Histological assessment

Figure 8A shows a complete rabbit lumbar region exhibiting cartilaginous osteophyte formation at the AF puncture site 4 weeks after surgery. Figure 8B shows gross specimens of control and punctured IVDs. The intact disk exhibited a jelly-like NP rich in water and with a

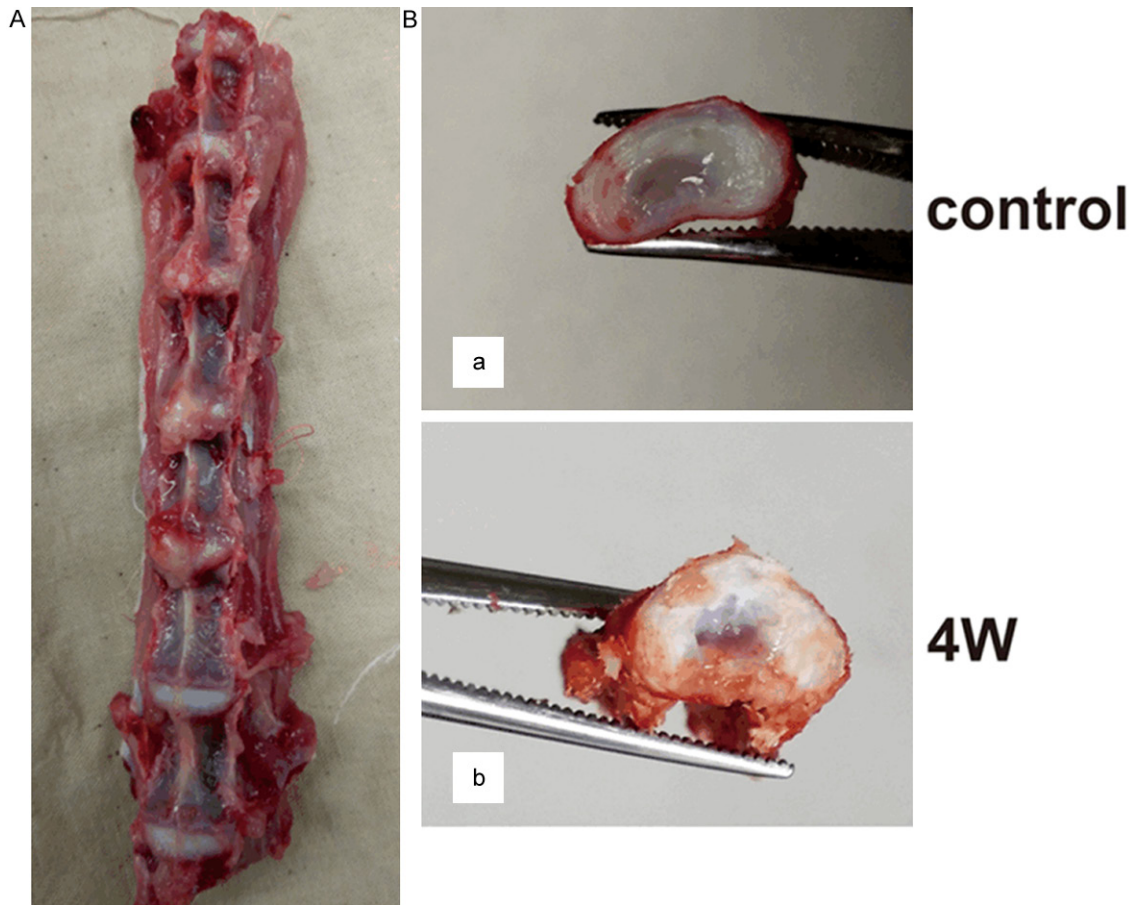


**Figure 8.** Gross specimen of a disc. (A) A complete rabbit lumbar region; (B) The intact disc (a) and the disc 4 weeks after puncture (b).

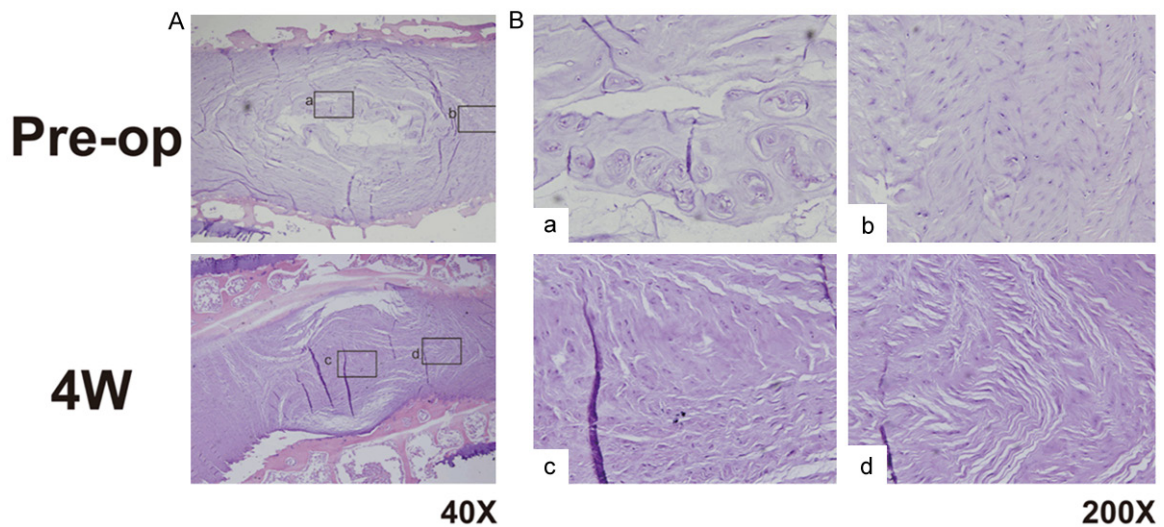


**Figure 9.** (A) representative histological sections of a healthy, intact rabbit lumbar disc and a disc 4 weeks after puncture (original magnification, 40 ×). (B) Magnified views of selected features of interest (original magnification, 200 ×). Before surgery, the NP displayed a mix of large, vacuolated (notochordal) cells and smaller, chondrocyte-like cells (a), and the AF was well organized (b). By 4 weeks after puncture, the NP demonstrated fewer notochordal cells and apparent chondrocyte-like cell proliferation (c). In addition, the AF had a wavy appearance, and the boundary between the NP and AF was not distinct (d).

## A novel method for establishing the degenerative IVD model

distinct definition between the NP and AF. In the punctured disc, the NP appeared viscous, and there was general loss of the border between the NP and AF.

**Figure 9** shows representative histological sections (stained with H&E) of a healthy, intact rabbit lumbar disc (i.e., a control disc) and a disc at 4 weeks after puncture by an 18-gauge lumbar needle. In the control disc, the NP exhibits a mix of large, vacuolated (notochordal) cells and smaller, chondrocyte-like cells. The AF was characteristically well organized with lamellar collagen sheets. The histology of the punctured disc revealed that by 4 weeks post-puncture, the NP exhibited fewer notochordal cells and apparent chondrocyte-like cell proliferation. A wavy appearance was evident in the AF, and the boundary between the NP and AF was not distinct.

### Discussion

IVD degeneration is a main cause of musculoskeletal disability in humans [17]. Biological treatment strategies to repair or regenerate degenerated IVDs appear promising as future therapeutic options [5]. Preclinical animal models of disease remain an important step in the translational development of novel biomedical technologies.

Numerous animal models of IVD degeneration have been proposed in the literature. The annular puncture model of IVD degeneration in rabbits is widely used and yields slowly progressive, mild, reproducible degeneration, similar to changes observed radiologically and histologically in human IVD degeneration [12]. Moss et al. [14] described in detail a retroperitoneal approach for establishing this model and provided a standardized protocol. In their opinion, this type of injury can often result in postoperative bilateral hind leg paralysis, and it is important to ensure the proper orientation of the needle during annular puncture; otherwise, the needle may injure the end plate, resulting in more rapid and severe IVD degeneration and introducing increased variability into the model. Additionally, an inappropriate direction can result in nerve root injury, and entering the spine canal can result in partial paralysis or self-mutilation of a dysesthetic area [14]. Zhang et al. [13] also noted that they incorrectly identified IVDs of interest during modeling. These

complications, in our experience, are likely due to the operative position, the deep operative incision, the obstruction of the transverse process and local muscle, and importantly, the lack of anatomical structures as references.

In the present study, the transabdominal approach we described can provide adequate IVD exposure. The L3/4 IVD can be localized precisely using the left renal vein, which was confirmed postoperatively by X-rays and MRI. We can easily ensure proper needle orientation under direct vision and avoid related complications occurring in the retroperitoneal approach. As observed postoperatively, all rabbits survived and maintained a normal diet. Their hind legs were not paralyzed, and the incisions healed well without becoming infected. Furthermore, the operation required approximately 20 min and resulting in less hemorrhaging. Most importantly, the animal model established via either the transabdominal or retroperitoneal approach is radiologically and histologically consistent with human IVD degeneration. The only attendant disadvantage of this approach is partial mild adhesion between the intestines and/or the abdominal wall; therefore, care must be taken to avoid injuring the intestines during any subsequent operations, which was shown to be feasible in the present study. Likewise, we do not recommend L2/3 disc or above as experimental objects because they are smaller, there are local complexities, and there is a lamellar cartilage osteophyte located in the front of the last thoracic vertebra to L2/3 disc anatomically.

Kroeber et al. [9] found that the discs could not recover once loading was removed after 28 days of loading in a new in vivo rabbit model created by axial compressive loading. In the rat tail model of disk degeneration, Inoue et al. [18] found that degenerated disks injected with recombinant human bone morphogenetic protein-2 at 4 weeks post-puncture exhibited temporarily improved disk grades according to MRI, whereas those injected at 6 and 8 weeks post-puncture did not. These findings suggest that the timing of biological treatments is critical and that they may be indicated in mild to moderate IVD degeneration because too much cell death has occurred in severe degeneration for these treatments to be effective without enough NP. As shown in **Figure 9**, there is a significant cartilaginous osteophyte anterior to the punctured IVDs, in which the NP exhibited vis-

cosity and atrophy. Thus, therapeutic factors administered at this point in disease progression may be ineffective. However, it is difficult to determine the best time for interventions. We graded the IVD degenerative degrees traditionally via radiological data observations, which inherently have observer error and bias. Recently, T2 relaxation time mapping was proposed as a quantitative technique for assessing early IVD degeneration [19, 20] and was shown to be related to both the glycosaminoglycan content and degeneration [21]. In our study, we found the T2 relaxation time could be used to quantitatively characterize grades I, II, and III rated by the modified Thompson classification system. However, more studies are warranted to determine the standard range of T2 values for the different grades and determine the best time for administering biological treatments.

The present study has some limitations. There were few experimental animals, and it was necessary to sacrifice some animals at intermediate stages for histology; hence, there was an unavoidable “dropout” rate over time.

### Conclusions

In conclusion, we provide an alternative approach for establishing the annular puncture model of IVD degeneration in rabbits. This approach is easy and can provide better visualization, consistent degeneration degrees and minimal complications. Notably, we could precisely identify the IVDs of interest using the left renal vein. Furthermore, we found that T2 mapping could discriminate grades of mild degeneration. This method has potential for enabling the determination of the optimal time for administering biological treatments.

### Acknowledgements

This work was supported by the National Natural Science Foundation of China (Grant No. 81272039).

### Disclosure of conflict of interest

None.

**Address correspondence to:** Zhengxue Quan, Department of Orthopedic Surgery, The First Affiliated Hospital of Chongqing Medical University, No. 1, Youyi Road, Yuanjiagang District, Chongqing 400-016, China. Tel: +86-023-89011212; Fax: +86-023-89011212; E-mail: quanxz18@126.com

### References

- [1] Hoy D, March L, Brooks P, Blyth F, Woolf A, Bain C, Williams G, Smith E, Vos T, Barendregt J, Murray C, Burstein R, Buchbinder R. The global burden of low back pain: estimates from the global Burden of disease 2010 study. *Ann Rheum Dis* 2014; 73: 968-974.
- [2] Luoma K, Riihimäki H, Luukkonen R, Raininko R, Viikari-Juntura E, Lamminen A. Low back pain in relation to lumbar disc degeneration. *Spine (Phila Pa 1976)* 2000; 25: 487-492.
- [3] Cook SD, Thomas KA, Harding AF, Collins CL, Haddad RJ Jr, Milicic M, Fischer WL. The in vivo performance of 250 internal fixation devices: a follow-up study. *Biomaterials* 1987; 8: 177-184.
- [4] Radcliff KE, Kepler CK, Jakoi A, Sidhu GS, Rihn J, Vaccaro AR, Albert TJ, Hilibrand AS. Adjacent segment disease in the lumbar spine following different treatment interventions. *Spine J* 2013; 13: 1339-1349.
- [5] An HS, Thonar EJ-MA, Masuda K. Biological repair of intervertebral disc. *Spine (Phila Pa 1976)* 2003; 28: S86-S92.
- [6] Singh K, Masuda K, An HS. Animal models for human disc degeneration. *Spine J* 2005; 5: 267S-279S.
- [7] Gruber HE, Johnson T, Norton HJ, Hanley EN Jr. The sand rat model for disc degeneration: radiologic characterization of age-related changes: cross-sectional and prospective analyses. *Spine (Phila Pa 1976)* 2002; 27: 230-234.
- [8] Lotz JC, Chin JR. Intervertebral disc cell death is dependent on the magnitude and duration of spinal loading. *Spine (Phila Pa 1976)* 2000; 25: 1477-1483.
- [9] Kroeber MW, Unglaub F, Wang H, Schmid C, Thomsen M, Nerlich A, Richter W. New in vivo animal model to create intervertebral disc degeneration and to investigate the effects of therapeutic strategies to stimulate disc regeneration. *Spine (Phila Pa 1976)* 2002; 27: 2684-2690.
- [10] Lü DS, Shono Y, Oda I, Abumi K, Kaneda K. Effects of chondroitinase ABC and chymopapain on spinal motion segment biomechanics. An in vivo biomechanical, radiologic, and histologic canine study. *Spine (Phila Pa 1976)* 1997; 22: 1828-1834.
- [11] Wei F, Zhong R, Zhou Z, Wang L, Pan X, Cui S, Zou X, Gao M, Sun H, Chen W, Liu S. In vivo experimental intervertebral disc degeneration induced by bleomycin in the rhesus monkey. *BMC Musculoskelet Disord* 2014; 15: 340.
- [12] Masuda K, Aota Y, Muehleman C, Imai Y, Okuma M, Thonar EJ, Andersson GB, An HS. A novel rabbit model of mild, reproducible disc degeneration by an annulus needle puncture:

## A novel method for establishing the degenerative IVD model

- correlation between the degree of disc injury and radiological and histological appearances of disc degeneration. *Spine (Phila Pa 1976)* 2005; 30: 5-14.
- [13] Zhang Y, Chee A, Shi P, Wang R, Moss I, Chen EY, He TC, An HS. Allogeneic articular chondrocyte transplantation downregulates interleukin 8 gene expression in the degenerating rabbit intervertebral disc in vivo. *Am J Phys Med Rehabil* 2015; 94: 530-538.
- [14] Moss IL, Zhang Y, Shi P, Chee A, Piel MJ, An HS. Retroperitoneal approach to the intervertebral disc for the annular puncture model of intervertebral disc degeneration in the rabbit. *Spine J* 2013; 13: 229-234.
- [15] Welsch GH, Trattng S, Paternostro-Sluga T, Bohndorf K, Goed S, Stelzeneder D, Mamisch TC. Parametric T2 and T2\* mapping techniques to visualize intervertebral disc degeneration in patients with low back pain: initial results on the clinical use of 3.0 Tesla MRI. *Skeletal Radiol* 2011; 40: 543-551.
- [16] Ogon I, Takebayashi T, Takashima H, Tanimoto K, Ida K, Yoshimoto M, Fujiwara H, Kubo T, Yamashita T. Analysis of chronic low back pain with magnetic resonance imaging T2 mapping of lumbar intervertebral disc. *J Orthop Sci* 2015; 20: 295-301.
- [17] Ferguson SJ, Steffen T. Biomechanics of the aging spine. *Eur Spine J* 2003; 12 Suppl 2: S97-S103.
- [18] Inoue H, Montgomery SR, Aghdasi B, Kaner T, Tan Y, Tian H, Terrell R, Wang JC, Daubs MD. The effect of bone morphogenetic protein-2 injection at different time points on intervertebral disk degeneration in a rat tail model. *J Spinal Disord Tech* 2015; 28: E35-E44.
- [19] Perry J, Haughton V, Anderson PA, Wu Y, Fine J, Mistretta C. The value of T2 relaxation times to characterize lumbar intervertebral disks: preliminary results. *Am J Neuroradiol* 2006; 27: 337-342.
- [20] Stelzeneder D, Welsch GH, Kovács BK, Goed S, Paternostro-Sluga T, Vlychou M, Friedrich K, Mamisch TC, Trattng S. Quantitative T2 evaluation at 3.0T compared to morphological grading of the lumbar intervertebral disc: a standardized evaluation approach in patients with low back pain. *Eur J Radiol* 2012; 81: 324-330.
- [21] Detiger SE, Holewijn RM, Hoogendoorn RJ, van Royen BJ, Helder MN, Berger FH, Kuijjer JP, Smit TH. MRI T2\* mapping correlates with biochemistry and histology in intervertebral disc degeneration in a large animal model. *Eur Spine J* 2015; 24: 1935-1943.